Modeling the Benefits of Vehicle-to-Grid Technology to a Power System

Yuchao Ma, Tom Houghton, Andrew Cruden, and David Infield, *Senior Member, IEEE*

***Abstract*—Electric vehicle (EV) numbers are expected to significantly increase in the coming years reflecting their potential to reduce air pollutants and greenhouse gas emissions. Charging such vehicles will impose additional demands on the electricity network but given the pattern of vehicle usage, the possibility exists to discharge the stored energy back to the grid when required, for example when lower than expected wind generation is available. Such vehicle-to-grid operation could see vehicle owners supplying the grid if they are rewarded for providing such services. This paper describes a model of an electric vehicle storage system integrated with a standardized power system (the IEEE 30-node power system model). A decision-making strategy is established for the deployment of the battery energy stored, taking account of the state of charge, time of day, electricity prices and vehicle charging requirements. Applying empirical data, the benefits to the network in terms of load balancing and the energy and cost savings available to the vehicle owner are analyzed. The results show that for the case under study, the EVs have only a minor impact on the network in terms of distribution system losses and voltage regulation but more importantly the vehicle owner's costs are roughly halved.**

***Index Terms*—Electric vehicle, power flow, state of charge, vehicle to grid.**

I. Introduction

UNTIL relatively recently, the potential introduction of electric vehicles (EV) has been viewed by electricity utilities as an additional load associated with battery recharging. Vehicle to grid (V2G) [1], [2] is a relatively new concept whereby the electric energy stored in the EV battery can also be fed back to the power grid. Initially, development of V2G technology was hampered by a conceptual doubt regarding the predictability of vehicle availability for charging/discharging since it depends on the specific behavior of each vehicle owner. However, where very large numbers of vehicles are involved and given the stochastic nature of vehicle usage, the aggregate level of load or power injection could be relatively well determined. Thus a cluster of vehicles could represent a well-defined responsive load or even a source of generation comparable in reliability to base load fossil-fuel power plants [2], [3]. The growing interest in electric vehicles is illustrated by a U.K. Department for Transport commissioned report which predicts that up to 1.5 million electric vehicles could be on the U.K. roads by 2020 [4]. Similarly, in the U.S., the California Air Resource Board's Zero Emission Vehicle Mandate suggested that 2 GW would be available by 2008 [5]. In the U.K., the estimated power available from the private automobile fleet is 1.98 TW based on an engine rating of 74.6 kW (100 HP) and 26.5 million registered vehicles [6]. The associated stored energy in the form of on board petrol reserves is roughly 7.7 TWh based on an average fuel tank size of 10 gallons being on average two thirds full. While this represents very much an upper bound on the potential storage available from battery EVs, since the range and power of EVs is expected to be lower than the internal combustion engined vehicles they replace, it nevertheless provides a useful benchmark. It is clear from this analysis that, if V2G enabled, these vehicles could offer significant generation capacity and opportunities for the provision of grid functionalities such as frequency response and peak lopping comparable in magnitude to those offered by current pumped storage hydroelectric schemes.

The application of battery storage to the provision of power system operational support and to improve local network performance is attracting increasing interest. Battery energy storage has been shown to be effective in suppressing fluctuations in power demand and providing frequency control and power quality support for decentralized power supplies as discussed by both Arita *et al.* and Sasaki *et al.* [7], [8]. Such systems can also provide local voltage control/support thus reducing the need for voltage regulation at distribution substations as investigated by Ohtaka and Wade *et al.* [9], [10]. The corollary of this is that the ability to provide network support services could also offer a revenue opportunity to EV owner/operators, further encouraging their adoption. The economic analysis of V2G technology as applied to current electricity markets has been widely studied in the literature. For example, Kempton and Tomic [11] calculate the effective generation capacity available from three types of EV and use this information to evaluate the revenue and costs for these vehicles if supplying electricity to three distinct markets: peak power, spinning reserves, and regulation. Zhong and Cruden [12] have made a similar assessment in the context of the U.K. electricity market, and a recent analysis has also been published by National Grid (the U.K. system operator) and Ricardo studying the U.K. V2G market [13].

This paper discusses how the energy stored in EVs might be most effectively utilized and presents an analysis of potential ap-

Manuscript received June 01, 2011; revised October 17, 2011; accepted November 03, 2011. Date of publication January 05, 2012; date of current version April 18, 2012. This work was supported by E.On via an International Research Initiative Award 2007. Paper no. TPWRS-00506-2011.

Y. Ma was with the University of Strathclyde, Glasgow G1 1XW, U.K., and is now with Vestas Technology R&D, Singapore (e-mail: yucma@vestas.com).

T. Houghton, A. Cruden, and D. Infield are with the University of Strathclyde, Glasgow G1 1XW, U.K. (e-mail: t.houghton@eee.strath.ac.uk; a.cruden@eee.strath.ac.uk; david.infield@eee.strath.ac.uk).

Color versions of one or more of the figures in this paper are available online at http://ieeexplore.ieee.org.

Digital Object Identifier 10.1109/TPWRS.2011.2178043

proaches to controlling the charging and discharging of parked EVs for power system support within the generic IEEE 30-node test system. Electricity power dispatch strategies are developed by the authors through the application of an aggregated model of the EVs and taking into account the vehicle battery capacity characteristics, state of charge, vehicle user driving habits and the electricity prices. Through the application of these strategies the EVs can be "instructed" to act as generation sources and/or as responsive loads depending upon the states of the power system and the EVs' battery storage system.

This paper is organized into six sections. A brief introduction to battery characteristics is presented in Section II. Section III describes the power system dispatch model with the integration of the EV battery energy storage. Dispatch strategies for battery storage power are developed in Section IV while numerical studies covering different test scenarios are conducted in Section V. Section VI provides concluding remarks on the applications of the V2G battery storage model.

II. Background, Battery Characteristics

Given a constant discharge current, any battery's state of charge (SoC), s, may be described with reference to its capacity by

$$s(t) = 1 - \frac{i_d t}{3600 C^a} \tag{1}$$

where

i_d discharge current in Ampere;

C^a available capacity in Ampere-hour (Ah);

t time in seconds.

According to the Peukert equation [14], the available capacity of the battery, C^a, is modeled as

$$C^a = \frac{i_d C^p}{(i_d)^k} \tag{2}$$

where

C^p Peukert capacity of the battery in Ah;

k Peukert exponent typically between 1.1–1.3.

Both C_p and k are fixed parameters with respect to a given battery. The Peukert capacity, C^p, is computed as

$$C^p = T\left(\frac{C^N}{T}\right)^k \tag{3}$$

where

C^N nominal capacity in Ah;

T rated discharge time in hour;

C^N/T the nominal discharge current in Ampere.

The value of the Peukert exponent in (2) and (3) for a specific battery can be derived by experimental test [12] and the lower the Peukert exponent, the better the performance of the battery ($k = 1$ is used to model the ideal battery). For a battery rated at 100 Ah for 5 h discharge time and a Peukert exponent of 1.2, the available capacity decreases from the 158.5 Ah to 87.1 Ah when the discharge current increases from 0.1 C/5 (2 A) to 2 C/5 (40 A), as shown in Fig. 1.

The battery no-load voltage is also a nonlinear dynamic variable. Fig. 2 shows the variation of voltage for different types of

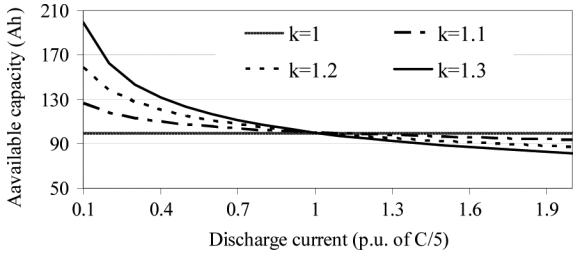

Fig. 1. Effective battery capacities at different discharge currents, 100 Ah at 5 h.

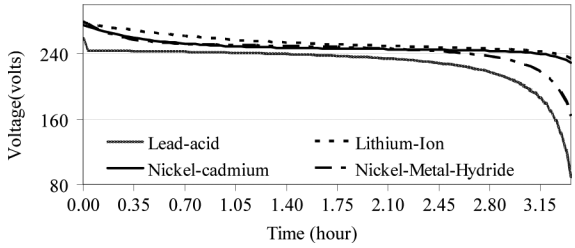

Fig. 2. Battery voltage versus time of use, for a range of 240 V /100 Ah, batteries at a discharge current of 1.5 C/5 (30 A).

TABLE I
Lookup the Battery Voltage versus Released Capacity, 240 Volts and 100 Ah, Lead-Acid Battery Type

Discharge /Charge Current		Voltage (volt) / Released capacity (Ah)							
(p.u.)	(A)								
0.1	2	259.4/0	244.6/20	…	237.5/60	…	225.4/80	…	123.2/100
…	…	…	…	…	…	…	…	…	…
0.5	10	258.9/0	244.2/20	…	237/60	…	224.9/80	…	122.8/100
…	…	…	…	…					
1.5	30	257.7/0	243/20	…	235.8/60	…	223.7/80	…	121.6/100

battery (all nominal values of 240 V, 100 Ah), at a discharge current of 1.5 C/5 (30 A) with respect to time.

To derive the charge/discharge energy during a specified time interval, the dynamic battery voltage must be first discretized by extracting the data from the discharge/charge curve of the battery. Since detailed information on the discharge/charge curves at different current levels for actual EV batteries is limited, this paper uses the simplified generic rechargeable battery model described by Tremblay, Dessaint, and Dekkiche [15]. A lookup table of voltage against released capacity at different discharge/charge currents has been built within the authors' model, as shown in Table I for a lead-acid battery.

Data in Table I are interpolated to derive the voltage corresponding to the updated SoC value at the beginning of the current time interval t, $s_{t\_}$, based on the selected discharge current i_d . Given the value of $s_{t\_}$, the released capacity until $t\_$, $C_{t\_}$, can be obtained from (1). Interpolation is then conducted to obtain the voltage value, $V_{t\_}$, based on the value of $C_{t\_}$. With the voltage $V_{t\_}$ and the current i_d, the discharge/charge power of the EV is obtained where the value of $V_{t\_}$ is assumed to be constant over the fixed time interval. The requirement to ensure

a constant voltage, and therefore constant power, over a fixed time interval is necessary for the subsequent power system load flow analysis.

Under the authors' proposed algorithm, the discharge/charge energy of the parked EV is controlled such that the SoC at the end of the time period t, s_{t+}, remains in the range $S_{\min}$ to $S_{\max}$ given the SoC, s_{t-}, at the start of the time period t. Generally, $S_{\min}$ is selected such that the EV will have sufficient energy to allow transportation to the next destination. The value of $S_{\max}$ meanwhile is set to avoid damage through overcharge.

III. Power Flow Model With the Integration of Battery Energy Storage

The steps required to obtain the battery storage power in a fixed time interval t are shown in the flowchart in Fig. 3 while the strategy for determining current, i_t, is described in the next section. The stored energy, EVP_t in Fig. 3, is not only constrained by the state of charge but will also be influenced by the driving requirements for the vehicles imposed by the user, e.g., the vehicle may be prevented from providing V2G service by the user because they have an extra journey to make. To put it another way, the bi-directional EV power flow possible to the power grid can be constrained either by the vehicle user driving profile or preference.

In Fig. 3

s_{t+} and s_{t-}	SoC values at the beginning and end of the current time interval t, respectively;
i_t	discharge or charge current of the EV during the time interval t;
C_{t-}	released capacity from the initial time to time point t_-.

One aspect of the driving profile is revealed through an analysis of the probability that a private car will be parked during a weekday, as shown in Fig. 4. This data is generated from time series analysis of the UK Time Use Survey (UKTUS) 2000 [16]. The probabilities are computed as the fraction of the approximately 26.5 million licensed cars [17]. Fig. 4 demonstrates two dips during the traffic rush hours from 07:00 to 09:00 and from 17:00 to 19:00 when most journeys occur. However, even during these rush hour periods at least 89% of private vehicles are parked. Although the vehicles taking part in the UKTUS are predominantly conventionally fuelled, the usage patterns are not expected to change dramatically with the shift to EVs, at least for shorter journeys. In calculating the number of parked cars that can be interfaced with the power grid, the model uses the probabilities shown in Fig. 4.

The other important aspect to consider is the likely journey distance to be travelled, or rather the amount of energy required to make that journey since this could vary according to driving conditions. Data from the Department for Transport [18] suggests that the average trip distance by private car is 8.4 miles. If the average range of an EV was considered to be 80 miles then in principle a minimum charge of roughly 10% would be sufficient to cover the average journey. However, the actual journey that the vehicle will take is not known to the network operator and

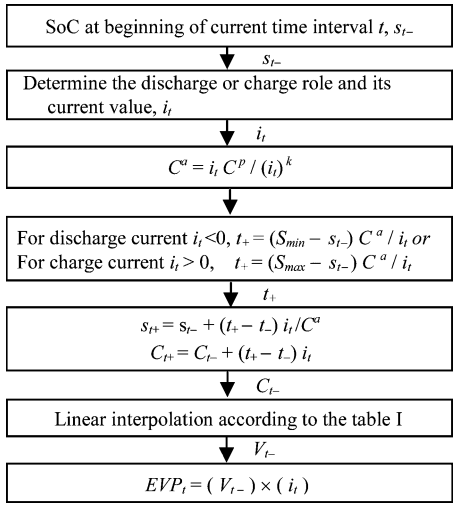

Fig. 3. Flowchart of deriving the battery storage power.

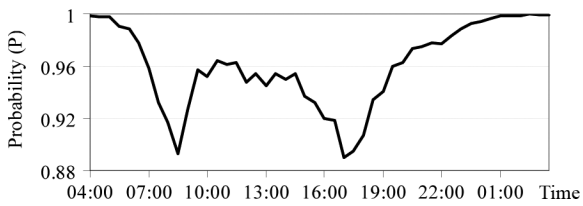

Fig. 4. Probability that private cars are not in use for transportation during a weekday.

indeed may not even be known to the vehicle driver who might be required to undertake an unexpected journey. Actual driving conditions might deviate from the average (due to a lack of real driving duty cycles for EVs, the energy consumed for on-road electric vehicles is assumed to be constant at the nominal level of 1 C/5 (20 A)) and in consequence a significantly higher minimum charge level, $S_{\min}$, is chosen to reflect these uncertainties.

In formulating the load flow model, the bi-directional power flow between the grid and the EVs, via a DC-AC power converter, is grouped and represented by a power injection at the bus to which it is connected. The power flow model is defined as

$$P_{n,t}\left(v_{1,t},\ldots,v_{n,t},\ldots,v_{N,t}\right) + \Sigma_e\left(EVP_{e,n,t}(i_e,t) * K_e^C\right) = 0 \quad \forall\, n \in N,\ e \in E \tag{4}$$

$$Q_{i,t}\left(v_{1,t},\ldots,v_{n,t},\ldots,v_{N,t}\right) = 0 \quad \forall\, i \in I \tag{5}$$

subject to

$$S_{e,\min} \le \left(s_{e,t-} + (t_+ - t_-)\frac{i_{e,t}}{C_e^a}\right) \le S_{e,\max} \quad \forall\, e \in E,\ t \tag{6}$$

$$V_i^{\min} \le |v_{i,t}| \le V_i^{\max} \quad \forall\, i \in I, \text{ for PQ load bus } i \tag{7}$$

$$Q_j^{\min} \le Q_{j,t} \le Q_j^{\max} \quad \forall j \in J \text{ for voltage controlled PV bus } j \tag{8}$$

where

E, N, I, J	set of EVs, power system buses, power system constant PQ load buses and voltage controlled PV buses such that $I + J = N - 1$;
e, t, n	index of individual EV, time interval and power system bus, respectively, e.g., $EVP_{e,t,n}(i_{e,t})$ indicates the battery power of EV e connected at bus n during the time interval of t, given the discharge/charge current of $i_{e,t}$;
t_-, t_+	beginning and end of the time interval t;
$s_{e,t-}, s_{e,t+}$	state of charge value of EV battery e at the time point t_- and t_+, respectively;
$P_{n,t}, Q_{i,t}$	real and reactive power balance at bus n at PQ bus i during the current time interval t, respectively;
$Q_j^{\min}, Q_j^{\max}$	lower and upper limits of the reactive power at voltage controlled PV bus j;
$v_{n,t}$	bus n voltage phasor value; $\mid v_{n,t} \mid$ is the magnitude value of $v_{n,t}$;
$V_n^{\min}, V_n^{\max}$	lower and upper limits of the voltage magnitude;
K_e^C	efficiency factor of the DC/AC converter.

IV. Battery Storage Power Dispatch Strategies

To ensure the battery SoC remains between $S_{\min}$ and $S_{\max}$ when the vehicle is connected to the grid, discharge and charge strategies need to be devised such that the amount of the power to be dispatched in any specified time period t does not violate the SoC constraints at the end of the current time interval t, i.e., to satisfy (6). A simulation time step of half an hour has been chosen to reflect the time step of current British Electricity Trading and Transmission Arrangements (BETTA) [19]. Three sets of rules, described below and expanded on in Fig. 5, are utilized when selecting the discharge/charge current, i_t from the predefined V2G operation options: namely low, medium and high levels, taking into account the SoC of the EVs and the half hourly electricity prices. In this paper, the limit values of $S_{\min}$ and $S_{\max}$ are set at 0.4 and 0.8 p.u., respectively, such that the battery discharge characteristics remain within the approximately linear section, which simplifies the required algorithm. It is worth noting that more robust analysis and definition of these limits is necessary, and is the subject of ongoing study by the authors. It is recognized that in practice battery performance may be adversely affected by such a charging regime [as most EV battery manufacturers require a full re-charge (to 100% SoC) and equalization (cell balancing) to maintain the warranty] and that a further iteration of the model may be required to allow the battery to be fully charged at least once per day.

Rule Set 1: The rule for setting the EV role, during the current time period t, EVR_t, is

$$SoC \geq 0.75 \rightarrow EVR_t = -1 \quad \text{(Discharge)} \tag{9}$$

$$SoC \leq 0.5 \rightarrow EVR_t = 1 \quad \text{(Charge)} \tag{10}$$

$$0.5 < SoC < 0.75 \rightarrow EVR_t = 2 \quad \text{(Undetermined)}. \tag{11}$$

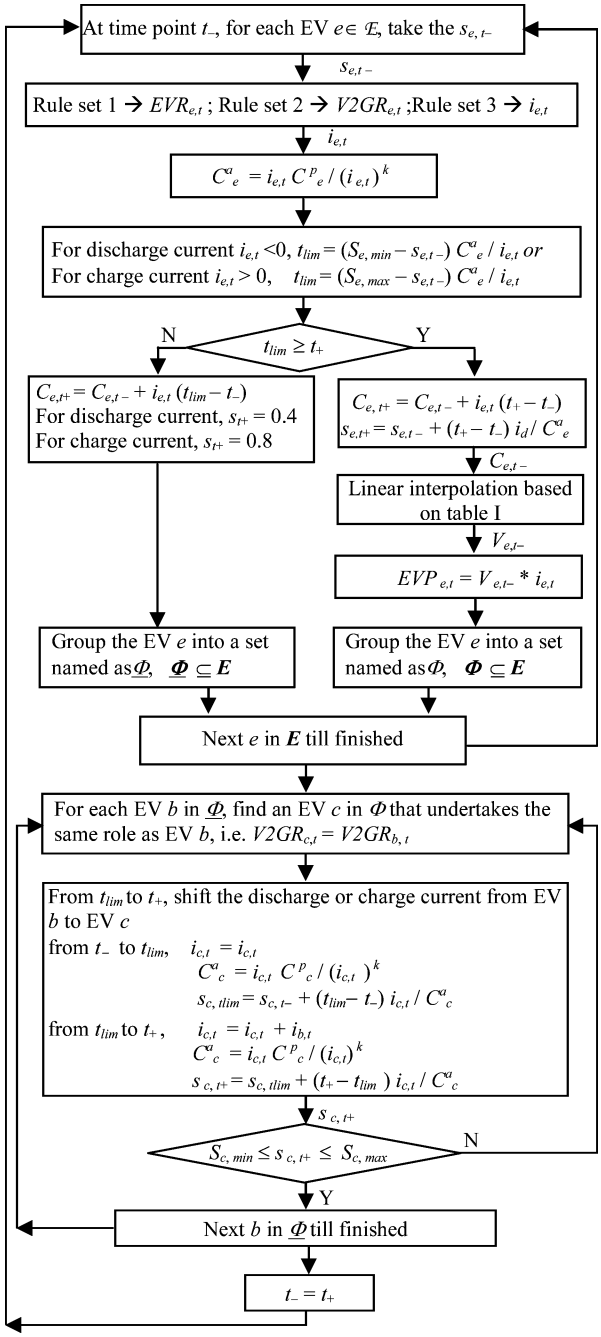

Fig. 5. Decision strategies of EV battery energy.

These limits for SoC, i.e., 0.5 and 0.75, are set to ensure that the gate values for $S_{\min}$ (0.4) and $S_{\max}$ (0.8) are not violated, although these specific limits are the subject of ongoing study by the authors.

Rule Set 2: An enable (1)/disable (0) control signal (CS) from a third party, such as an EV aggregator, is introduced to specify whether a vehicle is, in principle, available for V2G service. Whether a vehicle is in fact available for a V2G role during current time period t, $V2GR_t$, depends on both the control signal, CS, and SoC in Rule Set 1 as follows:

$$EVR_t = -1 \rightarrow$$

$$\text{If } CS_t = 1 \text{ then } V2GR_t = -1 \quad \text{(V2G service)} \tag{12}$$

$$\text{Else, } V2GR_t = 0 \quad \text{(Block off)} \tag{13}$$

$$EVR_t = 1 \rightarrow V2GR_t = 1 \quad \text{(Charge)} \tag{14}$$

$$EVR_t = 2 \rightarrow$$

$$\text{If } CS_t = 1, \text{ then } V2GR_t = 2 \quad \text{(Undetermined)} \tag{15}$$

$$\text{Else, } V2GR_t = 0 \quad \text{(Block off)}. \tag{16}$$

The value of CS enables (12) or disables (13) and (16) the V2G service. It is assumed the EV charging may be considered as a normal load on the system and can therefore be served regardless of the CS value, (14). In the case where the V2G role is undetermined by Rule Set 2, (15), the model invokes the electricity selling or buying price as defined by Rule Set 3.

Rule Set 3: The final rule used for selecting the level of discharge/charge current in time period t, i_t, reflects the prevailing price as follows:

Day time (from 08:00 to 00:00)

$$V2GR_t = 1 \rightarrow \tag{17}$$

$$\text{If } bpr_t \geq hbpr,\ i_t = I_L;\ \text{Else, } i_t = I_H$$

$$V2GR_t = -1 \rightarrow \tag{18}$$

$$\text{If } spr_t \geq hspr,\ i_t = -I_H;\ \text{Else, } i_t = -I_L$$

$$V2GR_t = 2 \rightarrow$$

$$\text{If } spr_t \geq hspr,\ i_t = -I_M$$

$$\text{Else if } bpr_t \leq hbpr,\ i_t = I_H$$

$$\text{Else } i_t = -I_L. \tag{19}$$

Night time t (from 00:30 to 07:30)

$$V2GR_t = 1 \rightarrow, \quad i_t = I_L \tag{20}$$

$$V2GR_t = -1 \rightarrow, \quad i_t = -I_L \tag{21}$$

$$V2GR_t = 2 \rightarrow, \quad i_t = -I_L \tag{22}$$

where

I_H, I_M, I_L	values of high, medium and low levels of the discharge/charge current. $+/-$ indicates the charge/discharge role;
bpr_t, spr_t	electricity buying price and selling price during current time period t, respectively;
$hbpr$, $hspr$	high electricity buying price and selling price, respectively.

Rule Set 3 is designed to take into account the price arbitrage opportunity, charging the EV at the high current rate when prices are low and discharging when prices are high (and if the V2G service is enabled), as defined in (17)–(19) for day time operation and (20)–(22) for night time operation. The values of $hbpr$ and $hspr$ form the threshold between low and high charge/discharge levels, and examining their influence on the final V2G results is the subject of continuing study by the authors. The possible undetermined value of the V2GR value in (15) is therefore determined by (19) and (22).

In Fig. 5, E is the set of EVs, $\underline{\Phi}$ is the set of EVs for which the state of charge constraints are violated during the current time interval and Φ is the complementary set of $\underline{\Phi}$, such that $\Phi + \underline{\Phi} = E$. The vehicles in set Φ are used as stand-by reserves for the vehicles in set $\underline{\Phi}$, provided that the paired vehicles (EV b and EV c in Fig. 3) take the same charge or discharge role during the time period. The energy is shifted from the vehicles in set $\underline{\Phi}$ that cannot be further charged, to the vehicles in complementary set Φ, in such a way as to maximize the utilization of the energy stored in the EVs within set Φ; thereby minimizing the impact on the network. A discharge/charge time limit, t_{lim}, is set according to the discharge/charge current, the actual state of charge at the start of the time period and the minimum/maximum state of charge as shown in (23) and (24):

$$t_{lim} = \frac{(S_{e,\min} - s_{e,t-})\, C_e^a}{i_{e,t}} \quad (\text{discharge, } i_{e,t} < 0) \tag{23}$$

$$t_{lim} = \frac{(S_{e,\max} - s_{e,t-})\, C_e^a}{i_{e,t}} \quad (\text{charge, } i_{e,t} > 0). \tag{24}$$

If t_{lim} is reached during the time period then instead of continuing to the end of the period charging continues until the time limit is reached and the simulator moves onto the next EV.

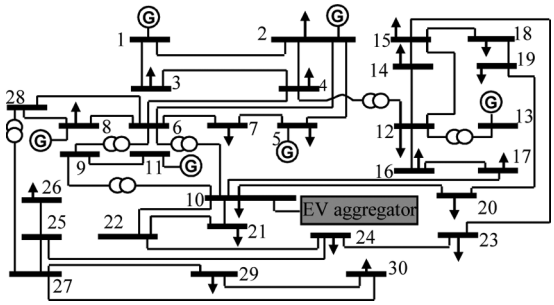

Fig. 6. EV aggregator connected to the IEEE 30-bus system.

V. Numerical Studies

The proposed EV energy storage model is applied to an IEEE 30-bus grid, the parameters of which are shown in Fig. 6 and are taken from Alsac and Stott [20]. The system comprises 132-KV, 33-KV, and 11-KV buses. The total load demand of the power system is based on a typical U.K. demand profile from Feb. 11/12 (from 04:00 to 03.30), 2010 [21], scaled by the maximal amount. An EV aggregator is introduced to represent a group of EVs that are connected at Bus 10 to the power system. In practice such a location could be a fleet charging and maintenance facility, or a terminus or vehicle parking area for a public transport provider. The modeling presented here focuses on privately owned electric cars, but in future electric busses for public transport could equally well be analyzed in a similar manner.

The characteristics of the EV batteries are listed in Table II and are applied to each individual EV within the same aggregation.

In Table II, the three options for the charge/discharge currents used in rule set 3, I_L, I_M, and I_H, can be defined as 0.1 C/5 (2 A), 0.5 C/5 (10 A), and 1.5 C/5 (30 A), where C is the rated capacity.

The EV on-road profile during one day is assumed to take one of three profiles reflecting differing degrees of EV take-up as shown in Fig. 7. Each profile is built up based on a total number of on-road vehicles of 1000, and the probability of being parked, P, as shown in Fig. 4. Due to a lack of real driving duty cycles for EVs, the energy consumed for on-road electric vehicle is

TABLE II
CHARACTERISTICS OF THE EV BATTERY IN SIMULATION

Battery Type	Rated Capacity (Ah)	Rated hours	Peukert exponent	Nominal Voltage (V)	Peukert Capacity (Ah)	Discharge /charge current p.u.of C/5	Effective Available capacity (Ah)
Lead-acid	100	5h	1.2	240	182.06	0.1	158.5
						0.5	114.87
						1.5	92.21

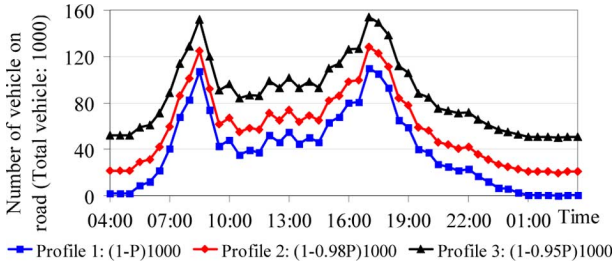

Fig. 7. Three profiles of electric vehicles on road during one day.

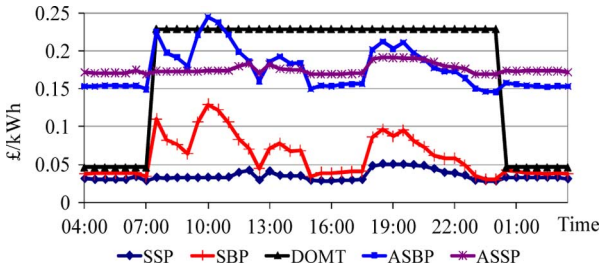

Fig. 8. Price profiles during one day (SSP/SBP: system selling/buying price [22], DOMT: domestic tariff, ASSP/ASBP: adjusted system selling/buying price.

assumed to be constant at the nominal level of 1 C/5 (20 A) discharge current.

In calculating the payments to and by the operator when the EVs are charged or discharged from the grid, the adjusted system selling price (ASSP) and adjusted system buying price (ASBP) values, as shown in Fig. 8, are introduced to reflect both the wholesale electricity prices and domestic tariffs. The ASSP values are computed by adding a margin, equal to the difference between the average tariff value and the average system selling price (SSP) value, to the SSP value at each time interval of one day. The same operation is applied to SBP values to get the ASBP. Since no established market pricing exists for EVs providing V2G services, existing system prices are used. The SSP and SBP values are taken from [22]. The high level of the ASSP price (£ 0.172/kWh) is set at 90% of the maximal ASSP (£ 0.191/kWh) whilst the high level of the ASBP price (£ 0.147/kWh) is set at 60% of the maximal ASBP (£ 0.245/kWh). It should be noted that the ASSP and ASBP values are specified at the power system operator side. These two values swap sense as the charging energy price (buying, ASSP) and discharging energy price (selling, ASBP) in calculating the payments to the EV and in applying decision rule set 3 as presented in Section IV.

Suppose the EV aggregator, with 1000 individual EVs, is connected at bus 10, as shown in Fig. 6 and the simulation run based

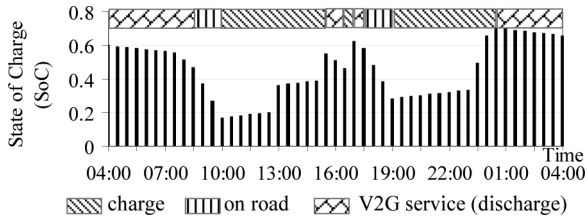

Fig. 9. State of charge of EV1 during one day.

on the EV on-road profile (Fig. 7). To explain the strategy decision process in Section IV in detail, an individual EV, EV1, is selected. EV1 is assumed to be on the road driving during two separate time intervals in a day, between 08:30 and 10:00 driving from home to the work place and between 17:30 to 19:00 returning home. During the other time periods EV1 is parked and plugged into the grid for charging or for providing V2G service. Based on the decision process in Fig. 5, the resulting SoC values for EV1 during one day are shown in Fig. 9.

The detail of the battery energy usage profile is reported in Table III. Between 04:00 and 08:30 EV1 provides V2G service with the battery being discharged at 0.1 C/5 (2 A) (rule (22)) until 07:30 and at 0.5 C/5 (10 A) between 07:30 and 08:30 due to the high electricity selling price (rule (19)) causing the SoC to decrease from 0.6 to 0.469. As mentioned previously, in a further iteration of the model a requirement to fully charge the battery at least once per day may be introduced. EV1 is on the road from 08:30 to 10:00, with the assumed discharge current of 20 A causing the SoC to decrease further to 0.169 at 10:00. From 10:00, EV1 is plugged back into the grid to be charged. The SoC increases slowly at first as the charging current is maintained at a low level owing to the high electricity buying price (higher than the high ASSP value of £ 0.172/kwh invoking rule (17)) prevailing between 10:00 and 12:30, as shown in Fig. 8. At 12:30 the ASSP falls to £ 0.170/kWh and the charging rate is ramped up to 30 A (rule (17)) and the SoC value increases quickly to 0.363.

Between 13:00 and 15:00 the ASSP again increases and the charging level reduces to 2 A, while a fall in price at 15:00 allows the charging current to be again increased to 30 A until a SoC of 0.551 is achieved at 15:30. From 15:30 to 16:30, EV1 provides V2G service at the 10 A level with the SoC decreasing to 0.464, after which it is charged at the 30 A current level from 16:30 to 17:00 to restore the SoC to 0.627. V2G service resumes between 17:00 and 17:30, at the 10 A level under rule (19) resulting in a final SoC of 0.583. EV1 is on the road from 17:30 to 19:00, discharging at the assumed rate and on arrival at the destination the SoC is 0.283. From 19:00 until 03:30 next day, the EV1 is plugged to the grid. EV1 gets charged from 19:00 to 00:30 and provides V2G service from 00:30 to 03:30.

For the group of vehicles, the cumulative payments and cumulative charge energy during one day are shown in Figs. 10 and 11, respectively. For the V2G service case, the payments and charge energy are £–1031.6 and 6675.1 kWh. Compared to the reference case where the EV is charged to recover the energy discharged in each journey (respecting the rules relating the electricity price and charging current), a cost saving of £ 1002,

TABLE III
BATTERY ENERGY STORAGE STATUS OF EV1

Time	Electr. buying price	Electr. selling price	SoC	Status	Time	Electr. buying price	Electr. selling price	SoC	Status	Time	Electr. buying price	Electr. selling price	SoC	Status
04:00	0.172	0.153	0.600	V2G service (2A) rule (22)	12:00	0.183	0.186	0.194	charge (2A) rule(17)	20:00	0.190	0.197	0.296	charge (2A) rule (17)
04:30	0.171	0.153	0.594		12:30:	0.170	0.160	0.200	charge (30A) rule (17)	20:30	0.189	0.189	0.302	
05:00	0.171	0.154	0.587		13:00	0.182	0.186	0.363	charge (2A) rule (17)	21:00	0.185	0.177	0.308	
05:30	0.171	0.154	0.581		13:30	0.176	0.193	0.369		21:30	0.180	0.173	0.315	
06:00	0.171	0.154	0.575		14:00	0.176	0.183	0.376		22:00	0.179	0.173	0.321	
06:30	0.174	0.154	0.568		14:30	0.176	0.184	0.382		22:30	0.176	0.164	0.327	
07:00	0.169	0.149	0.562		15:00	0.170	0.150	0.388	charge (30A) rule (17)	23:00	0.170	0.150	0.333	Charge (30A) rule (17)
07:30	0.173	0.225	0.556	V2G service (10A) rule (19)	15:30	0.169	0.154	0.551	V2G service (10A) rule (19)	23:30	0.169	0.146	0.496	
08:00	0.173	0.198	0.512		16:00	0.169	0.154	0.507		00:00	0.169	0.146	0.659	
08:30	0.173	0.192	0.469	on road	16:30	0.170	0.155	0.464	charge (30A) rule (17)	00:30	0.174	0.158	0.702	V2G service (2A) rule (22)
09:00	0.173	0.179	0.369		17:00	0.170	0.156	0.627	V2G service (10A) rule (19)	01:00	0.173	0.156	0.696	
09:30	0.173	0.221	0.269		17:30	0.171	0.157	0.583	On road	01:30	0.174	0.154	0.690	
10:00	0.174	0.245	0.169	charge (2A) rule (17)	18:00	0.189	0.202	0.483		02:00	0.174	0.154	0.683	
10:30	0.174	0.238	0.175		18:30	0.191	0.212	0.383		02:30	0.174	0.152	0.677	
11:00	0.174	0.221	0.181		19:00	0.191	0.203	0.283	charge (2A) rule (17)	03:00	0.173	0.153	0.671	
11:30	0.180	0.198	0.188		19:30	0.191	0.211	0.289		03:30	0.172	0.153	0.664	

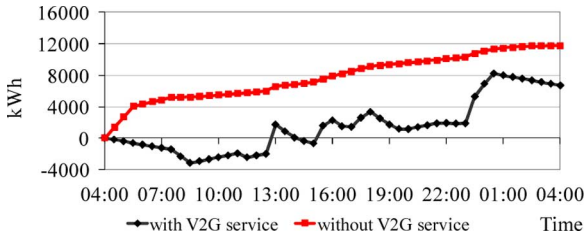

Fig. 10. Total cumulative net charge energy to the EV aggregator.

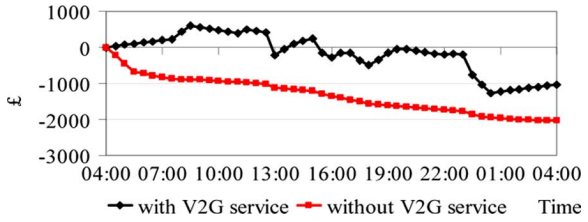

Fig. 11. Total cumulative payments from the EV aggregator.

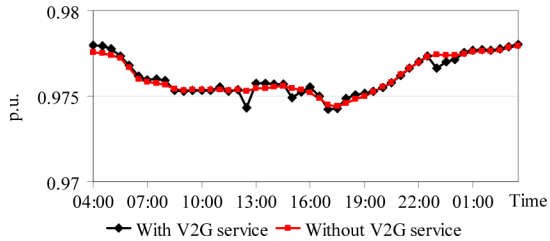

Fig. 12. Voltage magnitude at the EV-aggregator-connected bus 10.

or nearly 50%, is apparent, while the saved energy is significant at 5087 kWh.

With the introduction of the V2G service at bus 10 specifically, the power flow is simulated and the voltage magnitude at bus 10 and the total energy flow loss during one day, are shown in Figs. 12 and 13, respectively. It is observed from Fig. 12 that the voltage magnitude difference between the two cases is negligible due to the limited capacity share (7.2 MW in the most extreme case where all the 1000 EVs are either simultaneously discharged or charged at 30 A) compared with the overall system load (180 MW of lowest demand level). Regarding to the cumulative energy distribution losses, in the case where V2G service is provided, slightly less energy is lost (190 kWh in one day) on the transmission network compared with the reference case (Fig. 13). This is due to, and can be affected by, the geographical location, i.e., busbar, where the EVs are connected, as well as the control strategy of V2G service as explained in Section IV.

Tables IV and V report the simulation results under different cases. In Table IV Cases 1 to 3 are identical except for the vehicle-on-road profiles utilized which is all variations of the profile shown in Fig. 7. As the number of vehicles travelling in a given day increases from cases 1 to 3, the saved cumulative net charge energy and payments under V2G service increase from £ 1002 and 5087 kWh in case 1 to £ 1137 and 6012.7 kWh in case 2 and £ 1271.7 and 6974.6 kWh in case 3. Case 4 has three EV aggregators connected at the 11 KV buses 9, 11, and 13, respectively. Each aggregator has 5000 identical EVs except that the batteries of the EVs at bus 11 is assumed to be Lithium-Ion while the battery type of EVs connected at bus 13

TABLE IV
EV BATTERY ENERGY STORAGE RESULTS UNDER DIFFERENT TEST CASES

Test case	Total Vehicles	On road Profile	Location	Vehicle battery characteristics	Cumulative charge energy kWh with-/without-V2G(KWh)	Cumulative payments (£) with-/without-V2G-service
1	1000	1	bus 10	Table II	6675.1/11761.8	-1031.6 / -2033.2
2	1000	2	bus 10	Table II	8350.1 / 14362.8	-1343.9/ -2481.1
3	1000	3	bus 10	Table II	10953.6 / 17928.2	-1822.7 / -3094.4
4	5000	1	bus9	Table II	129528.5/ 220232.3	-20916.9/ -38033.6
	5000	2	bus11	Table II Lithium-Ion Battery		
	5000	3	bus13	Table II Nickel-Metal-Hydride Battery		

TABLE V
POWER SYSTEM OPERATION RESULTS UNDER DIFFERENT TEST CASES

Test case	Voltage at	Maximum daily value with-/without-V2G-service (upper limit value) p.u.	Minimum daily value with-/without-V2G-service (lower limit value) p.u.	Total daily energy loss with-/without-V2G-service (MWh)
1	bus 10	0.978/0.9779(1.05)	0.9742/0.9744(0.95)	104.24/ 104.43
2	bus 10	0.978/0.9779(1.05)	0.9743/0.9744(0.95)	104.32/ 104.56
3	bus 10	0.978/0.9778 (1.05)	0.9743/0.9744(0.95)	104.45 / 104.73
4	bus 9	0.9782/0.97792 (1.05)	0.964/0.974(0.95)	115.456 / 114.386
	Reactive power at	Maximum value during one day With-/wo-V2G-service MVAR	Minimum value during one day With-/wo-V2G-service MVAR	
	bus 11	43.35 /38.29 (50)	36.1/36.21 (-10)	
	bus 13	46.9/40.89 (50)	38.31/38.61 (-10)	

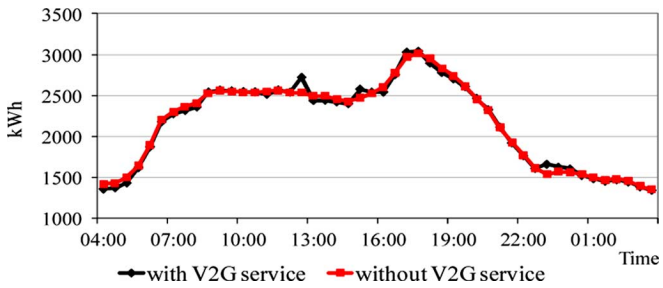

Fig. 13. Total energy loss profile.

is assumed to be Nickel-Metal-Hydride. Except for the dynamic voltage profiles which vary according to the Peukert Exponent, both the Lithium-Ion and Nickel-Metal-Hydride type of battery are assumed to have characteristics identical to those shown in Table II. Since the total capacity of the EVs in case 4 is 15 times that assumed for cases 1 to 3 and given the different battery configurations, the cumulative savings in terms of costs and charge energy under V2G service are £ 17,116.7, and 90.7 MWh, respectively. The impact of the V2G service from the EVs on the power system operation is summarized in Table V.

For case 4, bus 9 is a PQ bus while bus 11 and bus 13 are PV buses with voltage magnitude controlled at 1.05 p.u. Thus, the voltage magnitude at the PQ bus 9 and the reactive power requirements at PV buses 11 and 13 are required to be within the limit values during one day as discussed by Sasaki *et al.* [8] and Ohtada *et al.* [9]. The total energy flow loss of the IEEE 30-bus system is increased due to the V2G service, 1.07 MWh more than the case without V2G. However, taking into account the charge energy saved by the V2G service 90.7 MWh, there is an overall net saving of 89.6 MWh a day.

The authors are currently working on applying their V2G strategy to further network scenarios, both continuing with the IEEE 30 node model as well as the UK Generic Distribution System (UKGDS) network model [23].

VI. CONCLUSION

Electric vehicle batteries store energy when they are charged and release the energy when discharged. Apart from their intended main use for transportation, electric vehicles can serve as a rapid response load, or even as a generation source, for the power grid when they are parked, plugged into the grid and V2G enabled. However, the utilization of such storage energy from the electrical vehicle battery to power grid and vice versa is constrained by the battery state of charge and vehicle use requirements. To study this, the authors have developed a battery energy storage model for undertaking power system analysis within the recognized IEEE 30-bus test network.

With consideration of the state of charge constraints in charging and discharge cycles, a set of decision strategies has been formulated based on the battery power characteristics, electricity prices and vehicle usage requirements. Algorithms to deploy energy storage from electric vehicles have been developed and presented.

With reference to different test cases, the effects of the V2G service both on the individual EV and the power system operation has been investigated. The work of this paper has proved the feasibility of studying V2G through power flow analysis, and this will now be further developed to study the impact on low voltage distribution networks, where for instance V2G service might be used to support distribution system operation with attention to voltage control and congestion management, and also to firm up large penetrations of wind power into the power system as a whole. Furthermore, while it is considered that the results presented in this paper are robust, there is merit in performing a variety of sensitivity analyses as has been identified throughout the paper. This also forms part of the authors' ongoing work.

Results based on the U.K. market buy and sell price suggest that there is economic benefit to be had from V2G operation. In the specific cases considered, the vehicle aggregator could see roughly a halving of its costs, as shown in Fig. 7. Later work

will also consider the additional costs to deliver V2G services associated with the increased cycling of the batteries and an expected reduction in the battery life.

REFERENCES

[1] S. L. Andersson and A. K. Elofsson, "Plug-in hybrid electric vehicles as regulating power providers: Case studies of Sweden and Germany," *Energy Policy*, no. 38, 2010.

[2] W. Kempton and E. L. Steven, "Electric vehicles as a new source of power for electric utilities," *Transp. Res.*, vol. 2, no. 3, pp. 157–175, 1997.

[3] S. Huang and D. Infield, "The potential of domestic electric vehicles to contribute to power system operation through vehicle to grid technology," in *Proc. 44th International Universities Power Engineering Conf. (UPEC)*, Glasgow, U.K., 2009.

[4] Investigation into the Scope for the Transport Sector to Switch to Electric Vehicles and Plugin Hybrid Vehicles, Department for Transport, Oct. 2008. [Online]. Available: http://www.berr.gov.uk/files/file48653.pdf.

[5] W. Kempton and L. Tomic, "Vehicle-to-Grid Power: Battery, Hybrid, and Fuel Cell Vehicles as Resources for Distributed Electric Power in California, UCD-ITS-RR-01-03," 2001.

[6] Transport Statistics Great Britain 2007 Edition, Nov. 2007. [Online]. Available: http://www.dft.gov.uk/pgr/statist.ics/datatablespublications/tsgb/edition20071.pdf.

[7] M. Arita, A. Yokoyama, and Y. Tada, "Evaluation of battery system for frequency control in interconnected power system with a large penetration of wind power generation," in *Proc. Int. Conf. Power System Technology (PowerCon 2006)*, Oct. 22–26, 2006, pp. 1–7.

[8] T. Sasaki, T. Kadoya, and K. Enomoto, "Study on load frequency control using redox flow batteries," *IEEE Trans. Power Syst.*, vol. 19, no. 1, pp. 660–667, Feb. 2004.

[9] T. Ohtaka, A. Uchida, and S. Iwamoto, "A voltage control strategy with NAS battery systems considering interconnection of distributed generations," in *Proc. 2004 Int. Conf. Power System Technology (PowerCon 2004)*, Nov. 21–24, 2004, vol. 1, pp. 226–231.

[10] N. Wade, P. Taylor, P. Lang, and J. Svensson, "Energy storage for power flow management and voltage control on an 11 kV UK distribution network," in *Proc. 2009 20th Int. Conf. Exhib. Electricity Distribution*, Jun. 8–11, 2009, pp. 1–4.

[11] W. Kempton and J. Tomic, "Vehicle to grid fundamentals: Calculating capacity and net revenue," *J. Power Sources*, vol. 144, no. 1, pp. 268–279, Jun. 2005.

[12] X. Zhong and A. Cruden, "Assessment of vehicle to grid power as power system support," in *Proc. Smart Grid & Mobility Europe Conf.*, 2009.

[13] Bucks for Balancing: Can Plug-in Vehicles of the Future Extract Cash—and Carbon—From the Power Grid? National Grid and Ricardo joint White Paper. [Online]. Available: http://www.ricardo.com.

[14] J. Larminie and J. Lowry, *Electric Vehicle Technology Explained*. New York: Wiley, 2003.

[15] O. Tremblay, L. A. Dessaint, and A. I. Dekkiche, "A generic battery model for the dynamic simulation of hybrid electric vehicles," in *Proc. 2007 IEEE-Vehicle Power and Propulsion Conf.*, Sep. 9–13, 2007.

[16] The United Kingdom 2000 Time Use Survey Technical Report, 2003. [Online]. Available: http://www.statistics.gov.theme_social/UKTUS_TechRport.pdf.

[17] Vehicle Licensing Statistics: Transport Statistics Bulletin, 2008. [Online]. Available: http://www.dft.gov.uk/adobepdf/162469/221412/221552/228052/458127/vehic lelicensing2008.pdf.

[18] Department for Transport Statistics Database. [Online]. Available: http://www.dft.gov.uk/pgr/statistics/datatablespublications/tsgb/.

[19] British Electricity Trading and Transmission Arrangements (BETTA). [Online]. Available: http://www.nationalgrid.com.

[20] O. Alsac and B. Stott, "Optimal load flow with steady-state security," *IEEE Trans. Power App. Syst.*, no. 3, pp. 745–751, May 1974.

[21] UK national grid. [Online]. Available: http://www.bmreports.com/bwh_Indo.htm.

[22] UK national grid. [Online]. Available: http://www.bmreports.com/bsp/SystemPricesHistoric.htm.

[23] Details of the UK Generic Distribution System. [Online]. Available: http://www.sedg.ac.uk.

Yuchao Ma received the B.Sc. and M.Sc. degrees in electrical engineering from Chongqing University, Chongqing, China, in 1996 and 2002, respectively. In 2006, he received the Ph.D. degree in power systems engineering from Politecnic di Torino, Torino, Italy, supported by a full research sponsorship of the ECLEE project.

He worked as a post doctor research fellow from Politecnic di Torino and as a senior research scientist in Siemens Ltd., Corporate Technology, China, from 2006 to 2009. Then, he joined University of Strathclyde, Glasgow, U.K., as a research fellow in the Renewable Technology Group from 2009 to 2010. Currently, He is employed as a lead engineer in Vestas Technology R&D, Plant Systems Department. As chief author, he has published over 15 journal papers in power system engineering area. His research activities include wind power plant dynamic study and energy storage system integration solutions.

Tom Houghton received the M.Sc. degree in electrical engineering from Imperial College, London, U.K., in 1990, the M.B.A. degree from the London Business School in 1997, and the Ph.D. degree in renewable energy economics from the University of Strathclyde, Glasgow, U.K.

After receiving the Ph.D. degree, he worked as a post-doctoral research fellow at the University of Strathclyde, focused on economic simulation of renewable energy issues including transmission, generation, and end-user applications such as electric vehicles. Tom worked for Alstom in the turnkey power plants division as a project manager for more than 5 years and spent 8 years in the banking sector achieving the position of director in the Corporate Finance department of the Japanese investment bank Nomura. In addition to his research interests, he has established his own company in the renewable energy sector.

Andrew Cruden received the B.Eng. degree in electronic and electrical engineering, the M.Sc. degree in electrical power engineering, and the Ph.D. degree in the field of optical current sensing from the University of Strathclyde, Glasgow, U.K.

He has been a member of academic staff at the University of Strathclyde since 1998 and is currently a Reader within the Renewable Technology Group. His current research interests are: electrical energy storage, including investigation of vehicle-to-grid energy storage of aggregated electric vehicles; wind turbine condition monitoring; continuously variable transmissions for electric vehicles using magnetic gears. He has published over 100 journal and conference papers.

David Infield (SM'07) was born in Paris, France, in 1954 and raised and educated in England. He received the B.A. degree in mathematics and physics from the University of Lancaster, Lancaster, U.K., and the Ph.D. degree in applied mathematics from the University of Kent, Caterbury, U.K.

He worked first for the Building Services Research and Information Association (BSRIA) at Bracknell, Berkshire, U.K., and then for the Rutherford Appleton Laboratory in Oxfordshire, U.K., from 1982 to 1993, researching into renewable energy supplied electricity systems. From 1993 to 2007, he was with Loughborough University, Leicestershire, U.K., where he established CREST, the Centre for Renewable Energy Systems Technology. He is now a Professor of Renewable Energy Technologies with the Institute of Energy and Environment within the Department of Electronic and Electrical Engineering at the University of Strathclyde, Glasgow, U.K.

Dr. Infield is Editor-in-Chief of *IET Renewable Power Generation* and contributes to various IEC, CENELEC, and IPPC activities.